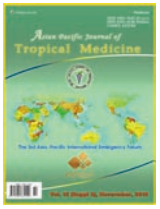

Original Article
Asian Pacific Journal of Tropical Medicine
journal homepage: www.apjtm.org

doi: 10.4103/1995-7645.271979 Impact factor:1.77

Feng-liao-chang-wei-kang is synergistic with 5-fluorouracil in inhibiting proliferation of colorectal cancer

Pan-li Ni[4], Shu-hong Tian[3], Zhao-xin Yang[3], Jun-qing Zhang[4], Fan Yang[3], Li-fan Zhong[4], Lian-fang Gan[4], Mian-qing Huang[3], Ling Huang[1,2,3]✉

[1]*Key Laboratory of Emergency and Trauma of Ministry of Education, Hainan Medical University, Haikou, Hainan 571199, P. R. China*

[2]*Key Laboratory of Preclinical Pharmacology and Toxicology of Hainan Province, Hainan Medical University, Haikou, Hainan 571199, P. R. China*

[3]*Research Center for Drug Safety Evaluation of Hainan Province, Hainan Medical University, Haikou, Hainan 571199, P. R. China*

[4]*School of Pharmaceutical Science, Hainan Medical University, Haikou, Hainan 571199, P. R. China*

ARTICLE INFO

Article history:
Received 26 September 2019
Revised 19 November 2019
Accepted 23 November 2019
Available online 3 December 2019

Keywords:
Colorectal cancer
FLCWK
5-fluorouracil
Synergistic effect
Colitis-associated colorectal cancer

ABSTRACT

Objective: To explore the effect of Feng-liao-chang-wei-kang (FLCWK) on acute and chronic gastroenteritis, synergistic effect on the growth inhibitory effect with 5-fluorouracil (5-FU) on colorectal cancer and its underlying mechanisms.

Methods: In the *in vitro* study, HT-29 cells were divided into 5-FU alone, FLCWK alone and coadministration groups. The MTT assay was used to analyze the proliferation of HT-29 cells at 24 h. Flow cytometry was used to observe the apoptosis, cycle of colorectal cancer HT-29 cells at 24 h. In the *in vivo* experiment, The subcutaneous transplantation tumor model of colorectal cancer HT-29-Luc was established with nude mice. All mice were randomly divided into 5-FU alone, FLCWK alone and coadministration groups according to body weight. During administration, the Interactive Video Information System small animal live imaging system was used to monitor the growth of subcutaneous transplantation in nude mice. The model of colitis-associated colorectal cancer (CACC) was established with BALB/c mice. BALB/c mice were randomly divided into the normal control group, the model control group, and the FLCWK group. At the end of the administration, the pathological status was detected by HE staining. Cell apoptosis of tumor tissue tumor and colon tissues were observed by TUNEL staining and TUNEL green fluorescence. The protein expression of Caspase 3, p-STAT3, Bcl-2, Bax and P-gp in tumor tissues tumor and colon tissues were tested by using immunohistochemical assay.

Results: FLCWK and 5-FU coadministration suppressed HT-29 cell viability and induced S phase arrest and apoptosis compared to treatment with 5-FU alone. Furthermore, compared to treatment with 5-FU alone, coadministration of FLCWK and 5-FU obviously reduced tumor volume and weight and induced apoptosis through decreasing p-STAT3 and P-gp and increasing Caspase 3 protein expression in a murine xenograft tumor model. Moreover, the result revealed decreased number and size of tumors following FLCWK protective administration, downregulated p-STAT3 and Bcl-2 levels and upregulated Bax and Caspase 3 expression in mice with CACC.

Conclusions: FLCWK has synergistic effects with 5-FU on colorectal cancer by suppressing the STAT3 pathway and downregulating P-gp expression. Furthermore, FLCWK administration suppresses CACC tumorigenesis by inhibiting the STAT3 pathway.

✉Corresponding author: Ling Huang, Key Laboratory of Preclinical Pharmacology and Toxicology of Hainan Province, Hainan Medical University, Haikou, Hainan 571199, P. R. China.
Tel:86-0898-66891789
Fax: 86-898-66893460
E-mail:Puer6@163.com
Funding project: This project was supported by the National Natural Science Foundation of China (No. 81760674 and No. 81403006).

How to cite this article: Ni PL, Tian SH, Yang ZX, Zhang JQ, Yang F, Zhong LF, et al. Feng-liao-chang-wei-kang is synergistic with 5-fluorouracil in inhibiting proliferation of colorectal cancer. Asian Pac J Trop Med 2019; 12(Suppl 2): 41-53.

1. Introduction

In the last ten years, colorectal cancer (CRC) has been one of the most frequently diagnosed malignant tumors[1] and has become one of the main reasons for cancer-related death in humans in the developed world[2,3]. Moreover, the 5-year survival rate of patients with advanced CRC is only 8%[4].

In addition to surgery, chemotherapy is a major therapeutic method for CRC[5]. The chemotherapeutic drug 5-fluorouracil (5-FU) is commonly used worldwide in the treatment of metastatic CRC[6,7]. However, the use of 5-FU is limited, mainly by its low chemotherapeutic efficiency. Due to multidrug resistance, the inhibition rate of 5-FU in CRC is only 20%–30%. Moreover, 5-FU may result in acquired resistance in cancer cells[8], leading to decreased chemotherapeutic efficiency. Therefore, novel and safe drugs are urgently needed to enhance the growth inhibitory effect of 5-FU on CRC.

P-glycoprotein (P-gp), a big transmembrane glycoprotein with a molecular weight of about 170 kD[9], is a drug efflux pump encoded by multidrug resistance 1 gene (*MDR1*) that removes drugs from cells against a concentration gradient. Overexpression of P-gp results in low intracellular drug concentrations, leading to drug resistance[10].

The transcription factor signal transducer and activator of transcription 3 (STAT3) is encoded by the *STAT* gene in humans[11]. A growing body of evidence indicates that constitutive activation of STAT3 signaling conduces to tumor progression and development in various human cancers, including colorectal cancer[12,13]. Interference with the STAT3 signaling pathway can inhibit cancer cell growth and induce apoptosis[14-18]. Furthermore, inhibiting gene expression of STAT3-mediated *MDR1* downregulates P-gp expression and transport activity, making inhibition of STAT3 a practical choice for the treatment of drug-resistant cancers. Therefore, STAT3 is believed as a promising anti-CRC drug[19].

Treatment of cancer with Traditional Chinese medicine (TCM) has a long history in China. TCM has been shown to increase the cytotoxicity of different anticancer drugs and to enhance the survival of cancer patients[20-24], suggesting that TCM agents may be promising therapeutic candidates to enhance effectiveness of chemotherapy for CRC.

Feng-liao-chang-wei-kang (FLCWK), a multi-component Chinese patent medicine, is composed of *Daphniphyllum calycinum* (family Daphniphyllaceae) and *Polygonum hydropiper* (family Polygonaceae) and has already gained extensive recognition in the treatment of acute gastroenteritis and chronic superficial gastritis in China[25,26]. The clinical application of FLCWK for many years has proven that it is a safe with high efficacy and has no obvious adverse effects. Our research team (C.N. Pat. No. 200510071092.3) confirmed that the main ingredients in FLCWK contain no less than 12% flavonoids, primarily quercetin, kaempferol, rutin, and isorhamnetin. As reported previously, flavonoids may decrease CRC risk[27-30].

Our previous study found that FLCWK can significantly inhibit *IL-6* and *STAT3* mRNA expression in rats model of ulcerative colitis. Moreover, we discovered that FLCWK suppresses P-gp transport activity in Caco-2 cells, which may provide a theoretical pharmacodynamic basis for the enhancement of 5-FU efficacy in CRC by suppressing the STAT3 pathway and downregulating P-gp expression.

In this study, we first investigated the effects of FLCWK in combination with 5-FU against CRC and the underlying mechanisms, focusing on the STAT3 pathway and P-gp expression. Additionally, we evaluated the potential protective effects of FLCWK in colitis-associated colorectal cancer (CACC) development and underlying mechanisms involving the STAT3 pathway.

2. Materials and methods

2.1. Materials and methods

FLCWK was purchased from Haikou Pharmaceutical Factory Co., Ltd. (Haikou, China). Fluorouracil injection was purchased from Tianjin Jinyao Pharmaceutical Co., Ltd. (Tianjin, China). Roswell Park Memorial Institute medium-1640 (RPMI-1640, C11875500BT) and high quality fetal bovine serum (FBS, #10099-141) were provided by Gibco; 0.25% trypsin (SH30042.01) and penicillin-streptomycin (SV30010) were obtained from HyClone. MTT powder (T100896) and DMSO (D103280) were purchased from Aladdin (Shanghai, China). The cell cycle and apoptosis detection kit (#340242) was purchased from BD Biosciences Pharmingen (San Diego, CA, USA). Azoxymethane (AOM) (A5486) was purchased from Sigma-Aldrich. Dextran sodium sulfate (DSS, #0218055880) with a molecular weight of 36 000–50 000 was purchased from MP Biochemicals (CA, USA). Rabbit monoclonal antibody against Bcl-2 (ab182858) and Bax (ab32503) was obtained from Abcam Company (Cambridge, UK). Rabbit monoclonal antibody against Caspase 3 (#9662) was obtained from Cell Signaling Technology (Beverly, MA, USA). rabbit polyclonal antibody against P-gp (22336-1-AP) was obtained from Proteintech (Wuhan, China) and Rabbit monoclonal antibody against p-STAT3 (P00007-3) was obtained from Boster Biological Technology (Wuhan, China). Annexin V-FITC Apoptosis Detection Kit (C1062M), One Step TUNEL Apoptosis Assay Kit (C1088) and Colorimetric TUNEL Apoptosis Assay Kit (C1098) were purchased from Beyotime (Shanghai, China). *D*-luciferin potassium salt (#122799) was purchased from PerkinElmer (Waltham, MA, USA). A general two-step detection kit (mouse/rabbit enhanced polymer system, pv-9000) was purchased from ZSGB-BIO Co., Ltd. (Beijing, China).

2.2. Cell culture

The human CRC cell line HT-29 was obtained from the Type Culture Collection of the Chinese Academy of Sciences (Shanghai, China). Cells were cultured in RPMI-1640 media supplemented with 10% FBS and 1% antibiotics at 37 ℃ in a humidified atmosphere with 5% CO_2 alone or in combination with HT-29 cell viability at 24 h.

2.3. Cell viability assay

The effects of FLCWK and 5-FU coadministration on HT-29 cell viability were examined using MTT assays. Briefly, cells were treated with different concentrations of (2.5, 5, 10, 20, 40, 80 and 160 μg/mL) FLCWK alone or in combination with 15 μM 5-FU, respectively. Following the treatment period, 10 μL of MTT working solution (5 mg/mL) was added to every well, and the cells were incubated for anymore 4 h at 37 ℃. The formazan crystals were dissolved by the addition of 150 μL DMSO after abandoning the supernatant. The absorbance of the solution at 570 nm was evaluated by a Bio-Rad ELISA reader.

2.4. Apoptosis assay

Apoptosis was measured by using a commercially available annexin V/PI-FITC cell apoptosis detection kit. Following the kit's instructions. HT-29 cells (1×10^6 cells/well) plated in 6-well plates were treated with 15 μM 5-FU alone or in combination with FLCWK (40, 80, and 160 μg/mL) for 24 h and collected. Then, the cells were stained with 10 μL propidium iodide (PI) and 5 μL annexin V-FITC through an annexin V-FITC/PI staining kit. The cells were incubated at room temperature for 15 min in the dark and then were analyzed by flow cytometry (BD Company, USA). Apoptosis was assessed in terms of the FITC-positive cells.

2.5. Cell cycle analysis

The cells plated in 6-well plates were treated with 15 μM 5-FU alone or in combination with various concentrations of FLCWK (40, 80 and 160 μg/mL) for 24 h. After treatment for 24 h, the cells were trypsinized, washed with phosphate-buffered saline (PBS), resuspended in 75% chilled ethanol, and stored overnight at 4 ℃. Then, the cells were washed with PBS, PI and RNase A stains were put in, the cells were incubated at 37 ℃ for 30 min in the dark, and cell cycle analysis was carried out using a flow cytometer (BD Company, USA).

2.6. Experimental animals

Forty-five male BALB/c mice and eighty-four BALB/c nude mice (18–22 g, five weeks old) were obtained from the Hunan SJA Laboratory Animal Co., Ltd. (Hunan, China) and placed in a particular pathogen-free environment at 22–24 ℃ with 40%–70% relative humidity and a light/dark cycle of 12/12 h.

2.7. Cell suspension preparation

The CRC cell line HT-29-Luc was obtained from Shanghai Aolu Biological Technology Co., Ltd. (Shanghai, China) and RPMI-1640 media supplemented with 10% FBS and 1% antibiotics at 37 ℃ in a humidified atmosphere with 5% CO_2. The cells were collected with 0.25% trypsin at the exponential growth stage and mechanically separated to gain cell suspension after centrifugation at 1 000 r/min for 5 min. The supernatant was abandoned, and normal saline (NS) was added to regulate the cell concentration to 1×10^7 cells/mL. We also assessed cell viability by 0.4% trypan blue exclusion assay (viable cells >90%).

2.8. Establishment of the transplantation tumor model and grouping

HT-29-Luc cells were transplanted by subcutaneous injection of 1×10^7 cells into the right flank of every nude mouse. Four days after transplantation, the mice were randomly allocated to the blank, model, FLCWK, low-dose 5-FU, FLCWK plus low-dose 5-FU, high-dose 5-FU and FLCWK plus high-dose 5-FU groups (n=12/group). The blank and model groups received NS by tail vein injection every other day and intragastric administration of sterile water every day, respectively. The FLCWK group received NS by tail vein injection every other day and intragastric administration of FLCWK (7.5 g/kg) every day. The low-dose and high-dose 5-FU groups received 5-FU (20 mg/kg and 25 mg/kg, respectively) by tail vein injection every other day and intragastric administration of sterile water every day. The FLCWK plus low-dose 5-FU group and FLCWK plus high-dose 5-FU group received 5-FU (20 mg/kg and 25 mg/kg, respectively) by tail vein injection every other day and intragastric administration of FLCWK (7.5 g/kg) every day. FLCWK was dissolved in sterile water and used immediately.

2.9. Bioluminescence imaging by the IVIS small animal live imaging system

Bioluminescence imaging was carried out using an Interactive Video Information System small animal live imaging system (Caliper Life Sciences, Hopkinton, MA, USA) on 0, 1, 4, 8, 12 and 17 days after treatment. Before imaging, *D*-luciferin potassium salt at 300 mg/kg body weight in 0.1 mL sterile PBS was administered by intraperitoneal injection. Finally, pseudo images were gathered by superposing emitted light over the grayscale photograph of the animal. Finally, quantitative image analysis was carried out with Living Image software (Caliper Life Sciences, Hopkinton, MA, USA).

2.10. Calculation of tumor volume and tumor inhibition rate

In this experiment, we measured the tumor twice a week and calculated the tumor volume (mm^3) by using the following formula:

$$\text{Tumor volume}=(W^2\times L)/2$$

W: width, L: length.

After 17 d of treatment, mice were anesthetized and killed by cervical dislocation. The tumors in each mouse in each group were excised and weighed. The tumor inhibition rate was computed by the following formula:

Tumor inhibition rate=(1-mean tumor weight of the treatment group/mean tumor weight of the control group)× 100%.

2.11. Generation and treatment of a mouse model of CACC

BALB/c mice were randomly divided into 3 groups (n=15/group): the normal control group, the model control group, and the FLCWK group. Adapted to a week later, the blank control group was intraperitoneally injected with NS, and the other groups were intraperitoneally injected with a single dose of AOM (12.5 mg/kg). After one week, 2.5% DSS was administered in drinking water for 7 days, followed by 14 d of regular drinking water; this process was repeated for a total of three courses. The dose of FLCWK administered to each mouse was calculated based on the standard clinical dose of 5 g/kg, and the mice in the FLCWK group were intragastrically administered 0.5 g/mL FLCWK once a day for 72 d to establish the mouse model of CACC.

2.12. Collection of animal tissue samples

The mice were anesthetized and killed by cervical dislocation on day 73 after model construction, their colons (from the ileocecal junction to the anal verge) were collected, and colon length was measured. Then, the colons were cut open along the main axis longitudinally and the colons were washed with PBS (pH 7.4) before the visual inspection to determine the mode of tumor development (including the location and quantity of every tumor inside the colon). The colonic tissues were fixed with 4% paraformaldehyde; stored with the remaining tissues at -80 ℃ in an ultralow temperature freezer for further use.

2.13. Histopathological assessment

For all animals, the excised tumor and colon tissues used for the histopathological examination were fixed overnight in PBS in 4% paraformaldehyde (pH 7.4). Paraffin-embedded tissue sections were stained with hematoxylin and eosin (H&E; for pathology evaluation).

2.14. TUNEL assay

TUNEL immunohistochemical assays and One Step TUNEL Apoptosis assays were conducted according to a previously described method[31,32]. Tissue sections (3 mm thick) were examined using the Colorimetric TUNEL Apoptosis Assay Kit following the protocol of the manufacturer. Simply, sections were dewaxed in xylene for 10 min and were digested with 20 mg/mL protease K excluded DNase at 37 ℃ for 30 min, Then, the sections were washed three times with PBS and incubated with 3% H_2O_2 in PBS for 20 min at room temperature. Washing the sections again 3 times with PBS and the sections were incubated with TdT enzyme solution for 60 min at 37 ℃. Subsequently, the sections were incubated in stop buffer for 10 min at 37 ℃ to terminate the reaction and incubated in Streptavidin-HRP working solution for 30 min at room temperature for color development, Finally, the sections were incubated with diaminobenzidine for 30 min at room temperature.

We also use A One Step TUNEL Apoptosis Assay Kit to assess apoptosis according to the manufacturer's instructions and the staining strength was gauged by fluorescence microscopy.

2.15. Immunohistochemical analysis

First, 3-mm-thick sections were dewaxed in xylene and gradually rehydrated in different concentrations of ethanol. Second, incubating the sections at 100 ℃ for 30 min in 10 mM citrate solution (pH 6.0) for antigen retrieval. A general two-step detection kit (mouse/rabbit enhanced polymer system) was used to conduct the immunohistochemistry (IHC) analysis according to the manufacturer's instructions. The sections were incubated with anti-Caspase 3 (1:100 dilution), anti-P-gp (1:200 dilution), anti-Bcl-2 (1:100 dilution), anti-Bax (1:200 dilution) and anti-p-STAT3 (1:50 dilution) antibodies at 4 ℃ overnight. Images were gained by using an optical microscope (OLYMPUS, BX41).

2.16. Statistical analysis

Statistical analysis was carried out by using GraphPad Prism 5 and SPSS17.0, and differences between groups were analyzed using one-way ANOVA. Data are represented as the mean±standard deviation (SD) and a P-value <0.05 was considered significant.

2.17. Ethics approval

The animal experiments were approved by the Experimental Animal Ethics Review Committee of Hainan Medical College (ERC application No.HY-2019-041, 11/18) and the research follows the ARRIVE guidelines.

3. Results

3.1. Effect of FLCWK and 5-FU coadministration on cell viability

MTT assays showed that treatment with 2.5 μg/mL to 160 μg/mL FLCWK alone showed no significant inhibition of HT-29 cell viability. However, the coadministration of 5-FU (15 μM) and FLCWK (2.5, 5, 10, 20, 40, 80 and 160 μg/mL) significantly increased the 5-FU-mediated inhibition of HT-29 cell viability compared with 5-FU alone (Figure 1).

3.2. Effect of FLCWK and 5-FU coadministration on apoptosis

The percentage of apoptotic HT-29 cells in the control group was (3.43±1.43)%. After administration with 5-FU alone or in combination with low-, medium- or high-dose FLCWK for 24 h, the percentages of apoptotic HT-29 cells were significantly increased (P<0.01). The results demonstrated that FLCWK synergized with 5-FU and had a dose-dependent effect on the apoptosis of HT-29 cells (Figure 2).

3.3. Effect of FLCWK and 5-FU coadministration on the cell cycle

As shown in supplementary Figure 1, the coadministration of 5-FU and low-dose FLCWK induced greater S phase arrest than 5-FU alone; the proportion of cells in S phase uncommonly increased from (14.70±1.74)% to (34.28±2.78)% after coadministration of 5-FU and medium-dose FLCWK compared to 5-FU alone (P<0.01). High-dose FLCWK in combination with 5-FU resulted in an enhance proportion of cells in the S phase compared with 5-FU alone (P<0.01). These findings indicated that FLCWK and 5-FU coadministration could increase S phase arrest and that this drug combination showed greater inhibition of HT-29 cell proliferation than 5-FU alone.

3.4. Effects of FLCWK and 5-FU coadministration on tumor growth inhibition by using xenogen bioluminescence imaging

Figure 3A demonstrates representative Xenogen imaging results from nude mice in different treatment groups. Figure 3B shows that the quantitative analysis data of Xenogen bioluminescence imaging on days 1 and 17. The average tumor size at the designated time point is represented as the imaging signal intensity (photons/second/cm^2/ser). The bioluminescence imaging data illustrated that compared with the model and FLCWK groups, the other treatment groups had significantly decreased tumor growth (P<0.05). Compared with the 5-FU 20 mg/kg group, the 5-FU 20 mg/kg+FLCWK group had significantly smaller tumors (P<0.05). In addition, compared with the 5-FU 25 mg/kg group, the 5-FU 25 mg/kg+FLCWK group also had significantly smaller tumors (P<0.05), which indicated that FLCWK increased the antitumor effects of 5-FU.

3.5. Effects of FLCWK and 5-FU coadministration on tumor size, tumor weight and tumor inhibition rate in the xenograft nude mice

The volume of HT-29 subcutaneous xenograft tumors in each group of nude mice increased to different degrees over 17 d (Figure 4). We observed the inhibitory consequent of FLCWK and 5-FU coadministration on tumor increase in nude mice and calculated the tumor inhibition rate. Figure 4A shows that the tumor volume was measured at intervals of 3-4 d. At the end of the experiment, we isolated and weighed all tumors from the xenograft nude mice. The tumor weights in the xenograft nude mice of the model, FLCWK, 5-FU 20 mg/kg, 5-FU 20 mg/kg+FLCWK, 5-FU 25 mg/kg, and 5-FU 25 mg/kg+FLCWK groups were (0.63±0.10) g, (0.65±0.12) g, (0.55±0.12) g, (0.46±0.05) g, (0.44±0.06) g and (0.34±0.07) g, respectively (Figure 4B). The final tumor weight of the FLCWK and 5-FU coadministration group was lower than that of the 5-FU alone group (P<0.05). The tumor inhibition rates of the FLCWK, 5-FU 20 mg/kg, 5-FU 20 mg/kg+FLCWK, 5-FU 25 mg/kg and 5-FU 25 mg/kg+FLCWK groups were 0%, 11.67%, 27.40%, 31.58% and 48.6%, respectively. The results illustrated that compared with those of the 5-FU alone groups, the tumor inhibition rates of the FLCWK and 5-FU coadministration groups were higher (P<0.05). These results suggested that FLCWK and 5-FU coadministration significantly inhibited tumor growth.

3.6. Effect of FLCWK coadministration with 5-FU on HT-29 xenograft tumor morphology

Figure 5 shows the results of H&E staining of tumors from each group. As seen in the figure, the tumor cells in the model group had various shapes, clear outlines, and intact cell membranes, and the nuclei of the cells in this group were round or oval, with different sizes, obvious nucleoli, and visible nuclear fission. At the same time, some tumor cells contained several nucleoli, and a few were apoptotic. In the low-dose 5-FU and low-dose 5-FU+FLCWK groups, some tumor cells had nuclear pyknosis and apoptosis; the number of apoptotic tumor cells in the high-dose 5-FU and high-dose 5-FU+FLCWK groups was relatively higher in the FLCWK and model groups. There were similar, and low levels of apoptosis were observed.

3.7. FLCWK and 5-FU coadministration induced apoptosis in xenograft tumor tissues

The effects of FLCWK and 5-FU coadministration on inducing apoptosis in HT-29 xenograft nude mouse tumor tissues were investigated by TUNEL staining. 5-FU alone induced little apoptosis in tumor tissues (Figure 6A), whereas coadministration of FLCWK and 5-FU strongly induced apoptosis.

3.8. FLCWK and 5-FU coadministration suppressed the STAT3 signaling pathway and P-gp expression in HT-29 xenografts

The mechanism underlying the suppression of *in vivo* tumor growth by FLCWK and 5-FU coadministration was investigated by immunohistochemical assays. The effect of FLCWK and 5-FU coadministration on STAT3 phosphorylation (p-STAT3), Caspase 3 and P-gp was examined in tumor tissues. As shown in Figure 6B-D, FLCWK and 5-FU coadministration reduced positive staining for p-STAT3 and increased positive staining for Caspase 3 in HT-29 tumors compared with 5-FU treatment alone. Furthermore, treatment with FLCWK alone or in combination with 5-FU significantly reduced positive staining for P-gp compared with 5-FU treatment alone.

3.9. Effect of FLCWK on the general activity and survival rate of mice with CACC

In the CACC model, the mice appeared to be weak with low activity, rough and dull fur, and symptoms such as diarrhea and bloody stools during the DSS challenge. After the DSS challenge was stopped, the mice gradually recovered from diarrhea and

bloody stools. As shown in Figure 7B, from the third cycle of model generation, the weight of the mice in the model control group significantly decreased, and more severe diarrhea and bloody stools were noticed, whereas the weight of the mice in the FLCWK group gradually increased. The general activity status in the FLCWK group was remarkably better than that in the model control group. According to the Kaplan-Meier survival curves (Figure 7C), FLCWK treatment improved mouse survival. The results showed that FLCWK can significantly enhance the general activity and survival rate of mice during the transition from inflammatory bowel disease to colon cancer.

3.10. Effect of FLCWK on tumor number and size and colon length in mice with CACC induced by AOM/DSS

Mouse colon tissues were dissected as previously described (Figure 7D). The colorectal mucosa of the normal control group was intact and smooth. But the mice in the model control group had high levels of viscous secretions from the anus and thickened intestinal mucosa, with a large number of densely distributed sizeable tumors that covered a vast area. By comparison, in the FLCWK group, there were fewer and smaller tumors, which were sparsely distributed within a smaller area. We also discovered that the number of tumors ⩾2 mm in diameter was obviously lower in the FLCWK group than in the model control group (P<0.05). The mouse colons were measured and compared among different groups (Figure 7F). The colon length was remarkably shorter in the model group than in the normal control group. The FLCWK group had a significantly longer colon than the model group (P<0.05). The results displayed that the administration of FLCWK can remarkably increase colon length in mice with CACC.

3.11. Effect of FLCWK on pathological changes in colon tissue of mice with CACC

H&E-stained sections of mouse colon tissues were observed under a microscope. As shown in Figure 7G, the colon tissues in the blank control group had normal structures, and the glands were arranged neatly. However, atypical hyperplasia invading the intestinal lumen was identified in the colonic mucosa of the model group. Tissues in this group appeared in the form of cauliflower with intact basement membranes and deep staining. The nuclei were enlarged with moderate nuclear allogeneic division, and inflammatory cell infiltration was evident. In the FLCWK group, nuclear pyknosis was identified in the proliferating mucosal epithelial cells. In addition, apoptosis, glandular enlargement, and increased levels of embedded necrotic materials were found.

3.12. FLCWK induced apoptosis in colon tissue of mice with CACC

The effects of FLCWK administration on the induction of apoptosis in colon tissue of mice with CACC were investigated by TUNEL staining. As shown in Figure 8E, the model group showed little apoptosis in colon tissues. However, the FLCWK treatment group presented relatively obvious apoptosis in colon tissues.

3.13. FLCWK reduced p-STAT3 and Bcl-2 levels and increased Bax and Caspase 3 expression in mice with CACC

To elucidate the mechanism by which FLCWK prevents CACC, we observed its effect on STAT3 and the downstream target genes *Bax* and *Bcl-2*. Immunohistochemical analysis showed that the amount of p-STAT3- and Bcl-2-positive cells in colon tissue sections was dramatically decreased after treatment with FLCWK, while Caspase 3 and Bax were upregulated in the FLCWK group compared with the control group, suggesting that FLCWK suppresses tumor growth in mice with CACC (Figure 8A–D). In general, our results indicated that STAT3 plays an important role in FLCWK-regulated Caspase-dependent mitochondrial apoptosis in mice with CACC.

4. Discussion

CRC is one of the most common cancers in the world and is the main reason for cancer-related death[33]. The drug 5-FU is one of the most commonly used chemotherapeutic agents in first-line treatment for CRC[34]. However, the clinical appliance of 5-FU is limited by its low chemotherapeutic efficiency. Therefore, there is a pressing need to identify valid drugs to enhance the growth inhibitory effect of 5-FU on CRC.

FLCWK, a traditional Chinese composite prescription, is known to be efficient and safe for the therapy of acute gastroenteritis and chronic superficial gastritis in China[25]. Notably, our previous study demonstrated that FLCWK can significantly inhibit *IL-6* and *STAT3* mRNA expression in a rat model of ulcerative colitis. Moreover, we discovered that FLCWK could suppress P-gp transport activity in Caco-2 cells. Therefore, we speculated that FLCWK may enhance the effects of 5-FU on CRC by suppressing the STAT3 pathway and downregulating P-gp expression.

In the present study, MTT assays were conducted to observe the effects of FLCWK and 5-FU coadministration on HT-29 cell viability. As expected, FLCWK and 5-FU coadministration can significantly decrease cell viability compared with 5-FU alone. Moreover, FLCWK and 5-FU coadministration uncommonly increased the number of apoptotic cells compared with 5-FU alone. Cell cycle data indicated that FLCWK and 5-FU coadministration increased S phase arrest compared to 5-FU alone, which affected the replication of cellular DNA and inhibited the division and proliferation of HT-29 cells.

Based on the above *in vitro* studies, we further evaluated the *in vivo* effect of FLCWK and 5-FU coadministration on CRC in the HT-29 xenograft mouse model. Our study showed that coadministration of FLCWK and 5-FU could significantly reduce tumor volume and

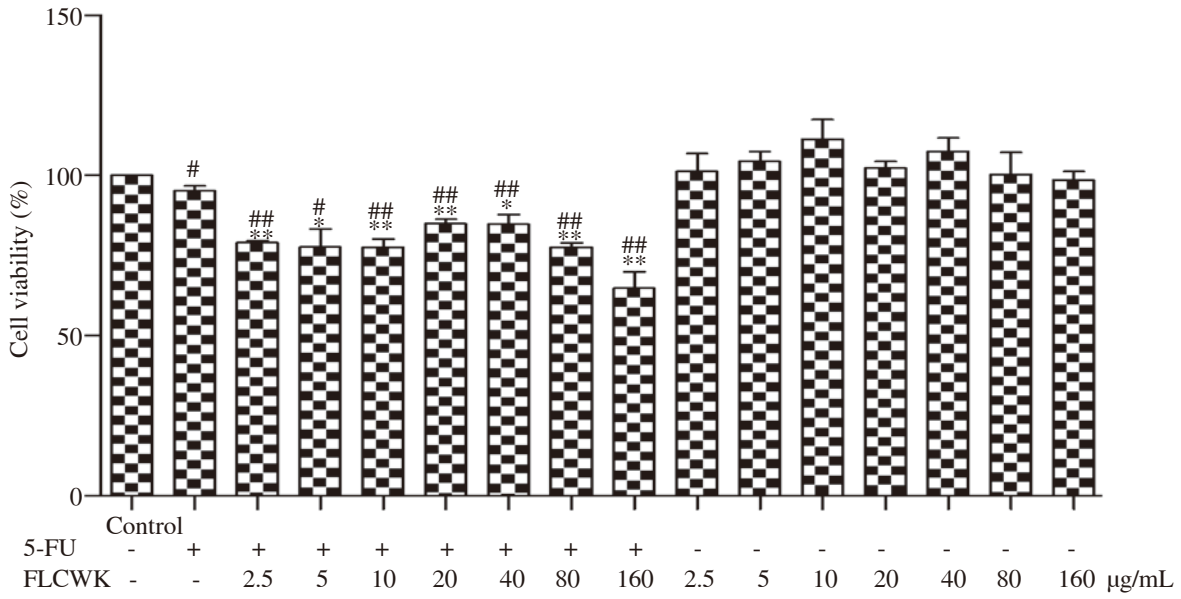

Figure 1. Effects of 15 μM 5-FU and different concentrations of FLCWK alone or in combination with HT-29 cell viability at 24 h. The results are shown as mean±SD of three independent experiments. $^{*}P$<0.05 compared to the 5-FU group, $^{**}P$<0.01 compared to the 5-FU group; $^{\#}P$<0.05 compared to the control group, $^{\#\#}P$<0.01 compared to the control group. FLCWK: Feng-liao-chang-wei-kang; 5-FU: 5-fluorouracil.

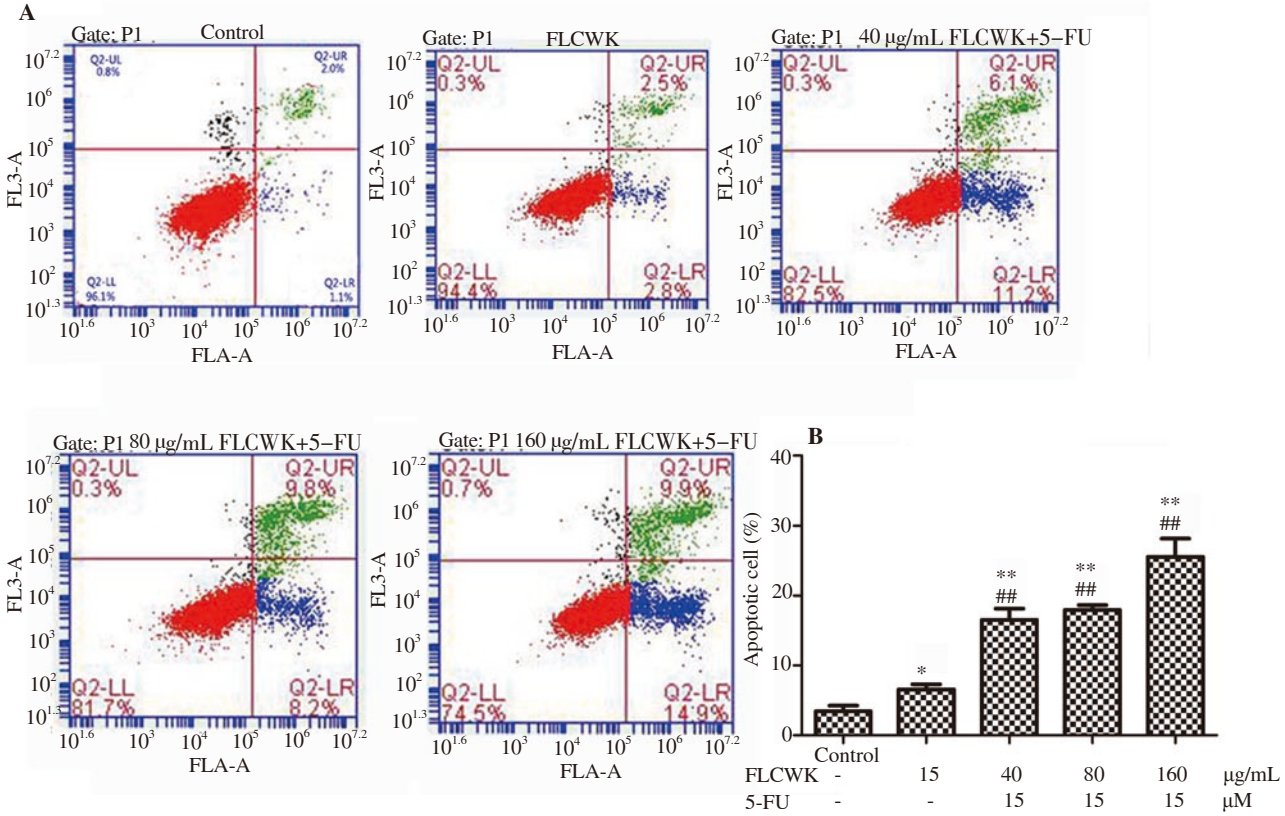

Figure 2. Effects of FLCWK on 5-FU-induced apoptosis. Apoptosis was measured using annexin V/PI staining followed by flow cytometric analysis. A: Typical scatter plots of annexin V (x-axis) *vs.* PI (y-axis) in every experimental group. B: Percent of apoptotic cells. Data are shown as the mean±SD of three independent experiments. $^{*}P$<0.05 compared to the control, $^{**}P$<0.01 compared to the control; $^{\#}P$<0.05 compared to the 5-FU group, $^{\#\#}P$<0.01 compared to the 5-FU group. FLCWK: Feng-liao-chang-wei-kang; 5-FU: 5-fluorouracil.

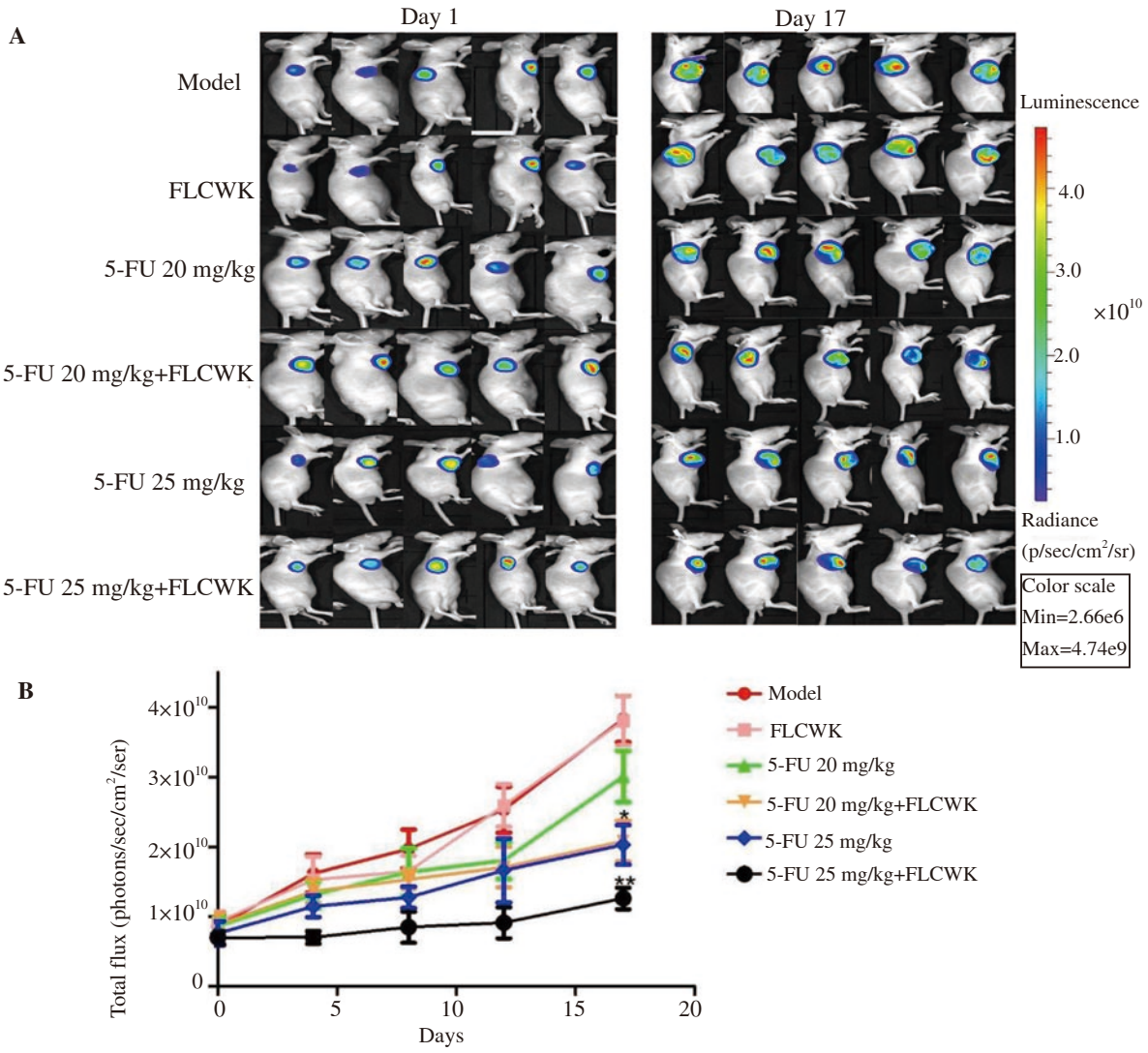

Figure 3. Effects of FLCWK and 5-FU coadministration on tumor growth inhibition by using xenogen bioluminescence imaging. Tumor growth was observed from day 1 (4 days after human colorectal cancer cell HT-29-Luc vaccination) to day 17. A: Representative Xenogen imaging results from xenografted nude mice in different treatment groups. B: Quantitative analysis of Xenogen bioluminescence imaging data. The average tumor size at the designated time point is illustrated as the imaging signal intensity (photons/second/cm^2/ser). n=12/group. Data are shown as mean±SD. $^*P$<0.05 compared to the 5-FU 20 mg/kg group, $^{**}P$<0.05 compared to the 5-FU 25 mg/kg group. FLCWK: Feng-liao-chang-wei-kang; 5-FU: 5-fluorouracil.

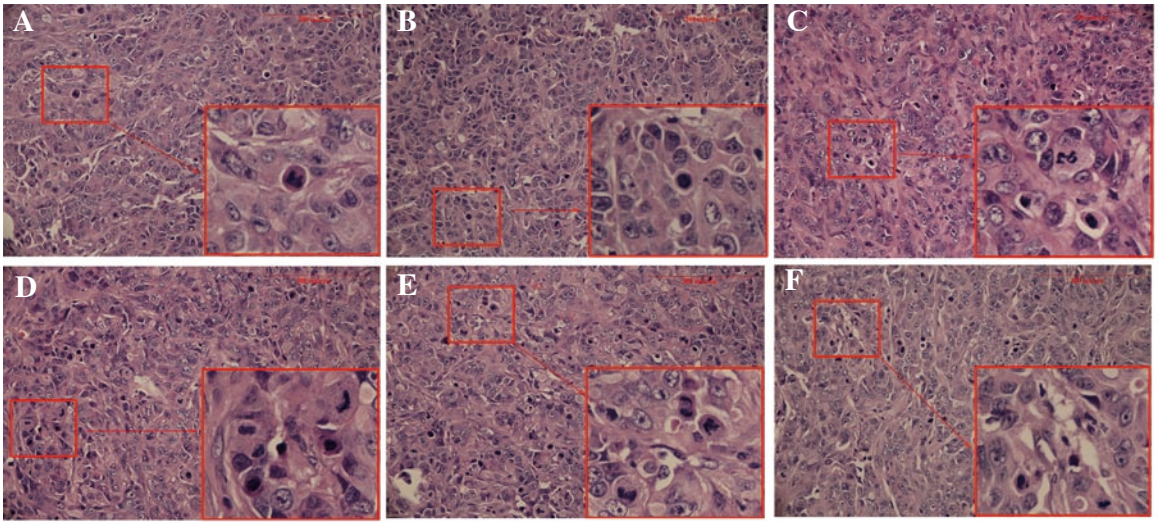

Figure 5. Results of H&E staining of HT-29 xenograft tumor tissues (scale bar:300 μm, 200×). A: model; B: FLCWK; C: 5-FU 20 mg/kg; D: 5-FU 20 mg/kg+FLCWK; E: 5-FU 25 mg/kg; F: 5-FU 25 mg/kg+FLCWK. FLCWK: Feng-liao-chang-wei-kang; 5-FU: 5-fluorouracil.

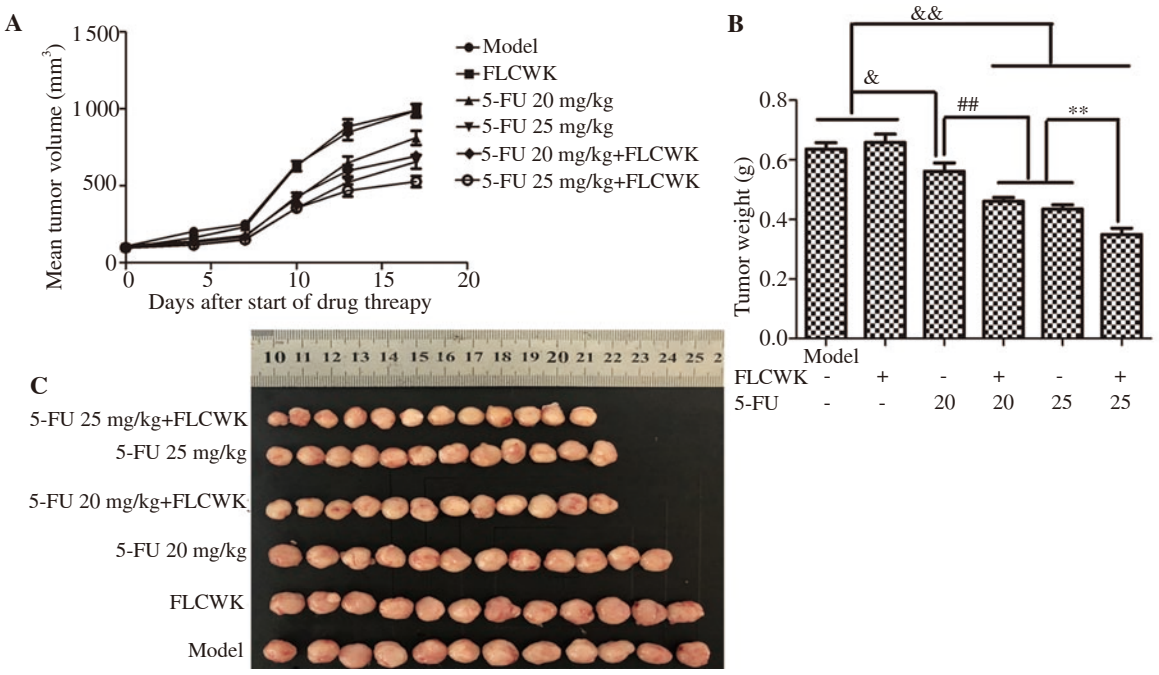

Figure 4. Effects of FLCWK and 5-FU coadministration on tumor size, tumor weight and tumor inhibition rate in the xenograft nude mice. A: Changes in tumor volume from day 1 to day 17. B: Changes in tumor weight. C: Photographs of xenografted athymic mouse tumors after the 17-day treatment. Data are shown as mean±SD. &P<0.05 compared to model, &&P<0.01 compared to Model; $^{\#\#}P$<0.01 compared to 5-FU 20 mg/kg; $^{**}P$<0.01 compared to 5-FU 25 mg/kg. FLCWK: Feng-liao-chang-wei-kang; 5-FU: 5-fluorouracil.

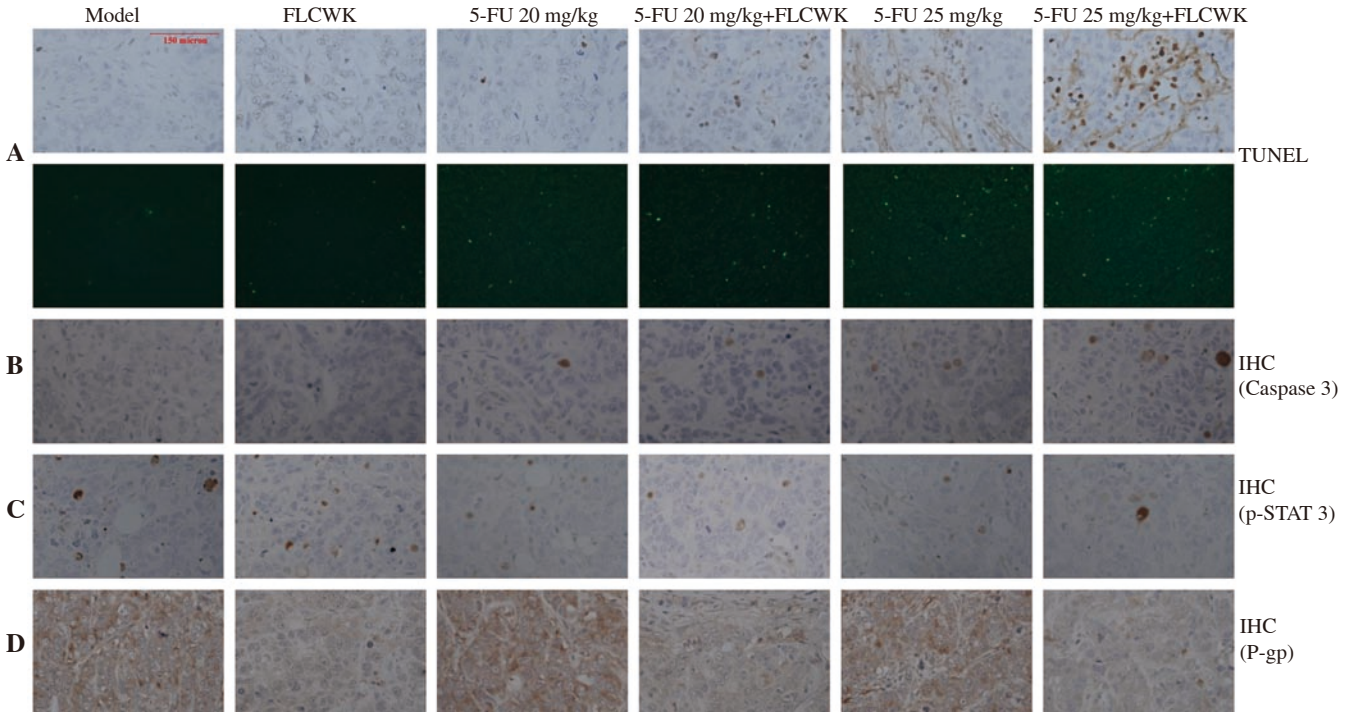

Figure 6. FLCWK enhances 5-FU-induced apoptosis in HT-29 colon tumors by suppressing the STAT3 pathway and downregulating P-gp expression. A: Apoptosis measured *via* TUNEL staining of tumor sections (scale bar:150 μm, 200×). Immunohistochemical analysis was adopted to analyze Caspase 3 (B), p-STAT3 (C) and P-gp (D) levels in tumor tissues secluded from mice treated under different conditions (scale bar:150 μm, 200×). FLCWK: Feng-liao-chang-wei-kang; 5-FU: 5-fluorouraci.

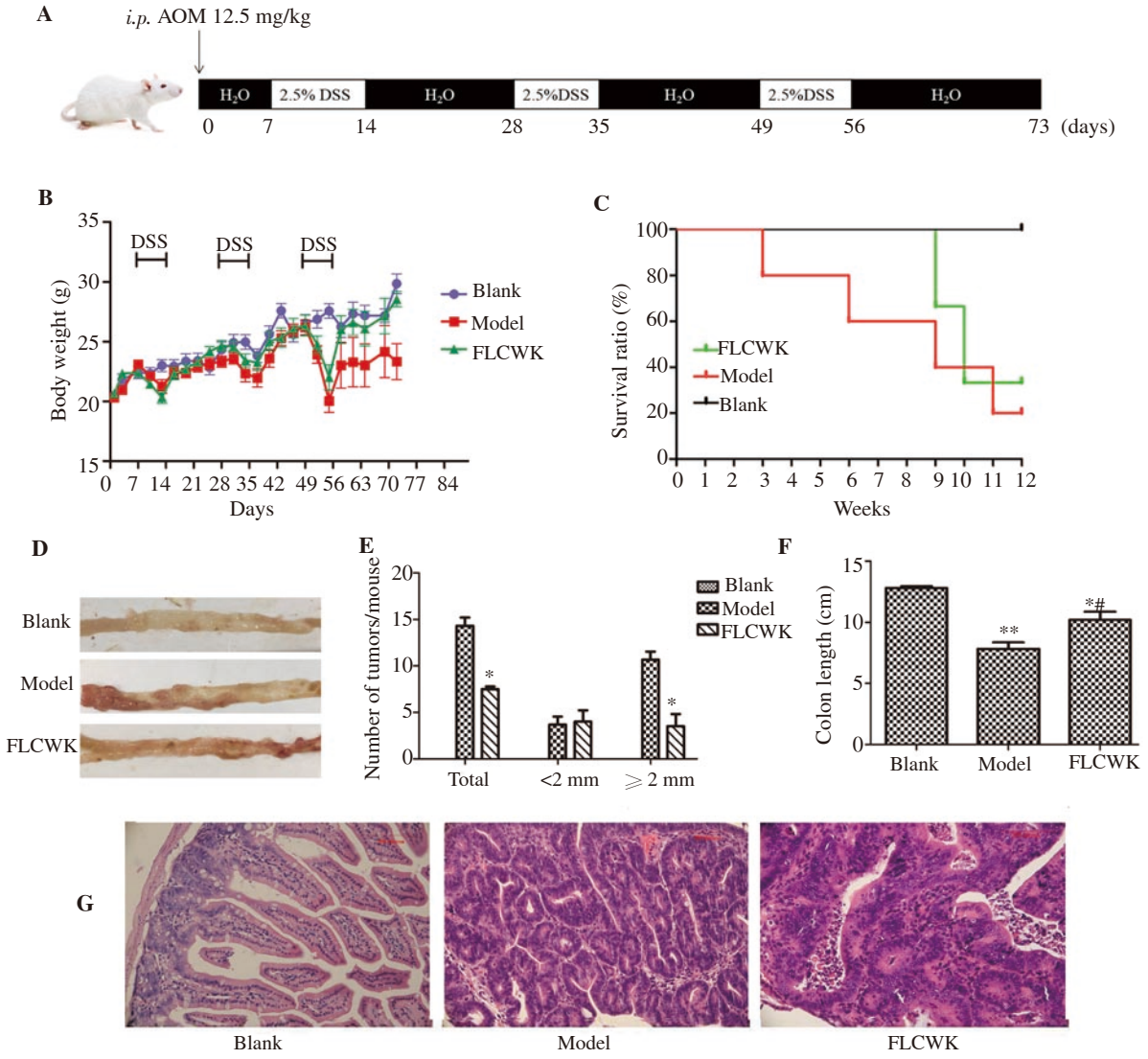

Figure 7. Preventive effect of FLCWK on colitis-associated colorectal cancer in BALB/c mice. A: The modeling process of CACC mice. B: Effect of FLCWK on mouse body weight. C: Effect of FLCWK on mouse survival ratio. D: Macroscopic view of the colons in mice with CACC. E: Amount of tumors in each group (n=3, $^{*}P$<0.05 compared with the model control group). F: Effect of FLCWK administration on colorectal length in mice with CACC. (n=3, $^{*}P$<0.05 compared to the blank group, $^{**}P$<0.01 compared to the blank group, $^{\#}P$<0.05 compared to the model control group). G: Effect of FLCWK on pathological changes in colon tissue in mice with CACC (scale bar: 300 μm, 200×). Data are shown as mean±SD. FLCWK: Feng-liao-chang-wei-kang.

weight compared to treatment with 5-FU alone. Additionally, the tumor inhibition rates in the FLCWK and 5-FU coadministration groups were higher than those in the 5-FU alone groups.

STAT3, a promising target for anticancer drug development, need phosphorylation (p-STAT3) on Tyr-705 for activation, which results in STAT3 transport into the nucleus to influence gene expression[35]. p-STAT3 levels play an important role in modulating the expression of key genes related in the monitoring of apoptosis, cell angiogenesis and proliferation[36]. IHC staining of xenograft tumor tissue indicated that the treatment of mice with FLCWK alone leads to no obvious change in positive staining for p-STAT3. Treatment with 5-FU alone or in combination with FLCWK decreased p-STAT3 levels in a dose-dependent manner. Notably, FLCWK and 5-FU coadministration decreased positive staining for p-STAT3 compared with 5-FU treatment alone.

Overexpression of P-gp in cancer cells can result in the efflux of anticancer drugs and made drug ineffectiveness, which is the main reason for tumor multidrug resistance[37]. IHC staining was also used to decide the expression of P-gp. Treatment with FLCWK alone or in combination with 5-FU significantly decreased P-gp expression levels compared with 5-FU alone. The results indicate that FLCWK and 5-FU coadministration suppresses tumor growth *in vivo* through the downregulation of P-gp expression.

Therefore, FLCWK could enhance tumor growth inhibition by 5-FU *in vivo* by suppressing the STAT3 pathway and downregulating P-gp expression. Notably, previous research has shown that inhibition of STAT3 activation can effectively reduce P-gp expression[37]. Thus, we hypothesized that the suppression of tumor growth *in vivo* by FLCWK and 5-FU coadministration might also be related to STAT3-regulated P-gp expression; this hypothesis requires further study.

Furthermore, we analyzed the influence of FLCWK and 5-FU

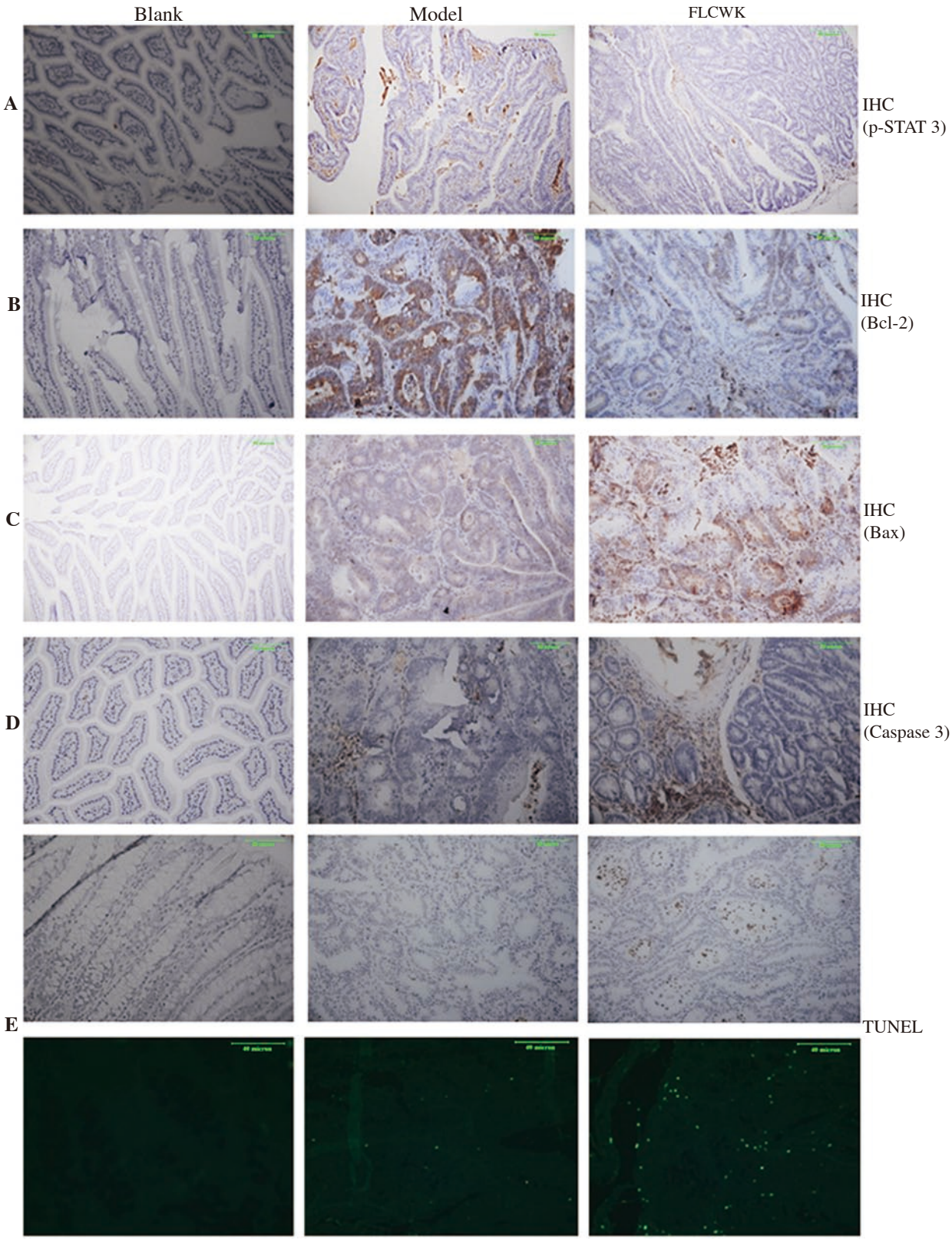

Figure 8. FLCWK promotes apoptosis in mice with CACC through suppressing STAT3 signaling pathways. Immunohistochemical analysis was adopted to analyze p-STAT3 (A), Bcl-2 (B), Bax (C), and Caspase 3 (D) levels in colon tissue separated from mice treated under different conditions (scale bar: 80 μm, 200). (E) Apoptosis was measured *via* TUNEL staining of colon sections (scale bar: 80 μm, 200× and 40 μm, 400×). FLCWK: Feng-liao-chang-wei-kang.

coadministration on apoptosis in the HT-29 xenograft mouse model. H&E and TUNEL staining affirmed an enhanced proportion of apoptotic cells in tumor tissue from mice cotreated with FLCWK and 5-FU. Of note, the *in vivo* apoptotic results were consistent with the *in vitro* results. Caspase 3, which is a member of the Caspase family, plays a key role in mitochondria-mediated apoptosis and contributes to apoptosis through the activation, hydrolysis, and proteolysis of particular substrates[38]. The results indicate that coadministration of FLCWK and 5-FU uncommonly upregulated Caspase 3 protein levels compared to treatment with 5-FU alone, implying that the apoptosis induced by FLCWK and 5-FU coadministration was closely related to Caspase 3 upregulation.

Additionally, we observed the potential protective effects of FLCWK on CACC development in BALB/c mice. Our findings revealed that FLCWK administration can improve the general activity and survival rate of mice with CACC and decrease the number and size of tumors in these mice. IHC analysis indicated that p-STAT3 levels were significantly reduced in the FLCWK-treated groups compared with the model group, indicating that FLCWK administration strongly inhibits tumorigenesis in mice with CACC through suppressing the STAT3 pathway.

We also observed the role of FLCWK on apoptosis in AOM/DSS-induced mice. H&E and TUNEL staining showed that FLCWK administration induced relatively obvious apoptosis in colon tissues. Normally, apoptosis occurs *via* the death receptor pathway and/or the mitochondrial pathway[39,40]. Bcl-2 family proteins are widely related in the mitochondrial pathway[41]. Notably, *Bcl-2* and *Bax*, which are *STAT3* target genes, maintain the balance of pro- and anti-apoptotic molecules. An elevated Bax/Bcl-2 ratio promotes apoptosis through the Caspase-dependent pathway[42-44]. Caspase 3 is an important component of the cell death machinery and is considered as the most downstream enzyme in the apoptosis pathway because of its location in the protease concatenation[45].

IHC analysis also showed that the amount of Bcl-2-positive cells in colon tissue sections was dramatically reduced after FLCWK administration, while Bax and Caspase 3 were upregulated in the FLCWK group compared with the control group, implying that FLCWK administration induced apoptosis in colon tissues through the Caspase-dependent mitochondrial apoptosis pathway.

In conclusion, this study demonstrated that FLCWK could enhance the growth inhibitory effect of 5-FU on CRC by suppressing the STAT3 pathway and downregulating P-gp expression. In addition, preventive FLCWK treatment could significantly suppress the development of CACC by suppressing the STAT3 pathway and induce apoptosis by activating the Caspase-dependent mitochondrial apoptosis pathway. Based on these findings, FLCWK is a novel candidate 5-FU adjuvant to improve the treatment efficiency of 5-FU on CRC and is a potential agent for the prevention and therapy of CACC.

Conflict of interest statement

The authors declare that they have no conflict of interest.

Funding project

This project was supported by the National Natural Science Foundation of China (No. 81760674 and No. 81403006).

Authors' contributions

H.L. conceived and designed the experiments. N.P. and Z.L. carried out the experiments. T.S. and G.L. analyzed the data. Z.J., Y.F. and H.M. contributed materials, reagents and analysis tools. Y.Z. wrote the paper. All authors read and authorized the manuscript and assent to take responsibility for all respects of the research in assurance that the integrity or accurateness of any part of the work are suitably investigated and solved.

References

[1] Siegel RL, Miller KD, Jemal A. Cancer statistics. *CA Cancer J Clin* 2018; **68**: 7.

[2] Marley AR, Nan H. Epidemiology of colorectal cancer. *Int J Mol Epidemiol Genet* 2016; **7**: 105-114.

[3] Siegel RL, Miller KD, Jemal A. Cancer statistics, 2017. *CA Cancer J Clin* 2017; 67(1): 7-30.

[4] Wu S, Qiu Y, Shao Y, Yin S, Wang R, Pang X, et al. Lycorine displays potent antitumor efficacy in colon carcinoma by targeting STAT3. *Front Pharmacol* 2018; **9**: 881.

[5] Fu Y, Yang G, Xue P, Guo L, Yin Y, Ye ZQ, et al. Dasatinib reduces 5-Fu-triggered apoptosis in colon carcinoma by directly modulating Src-dependent Caspase-9 phosphorylation. *Cell Death Discov* 2018; **4**: 61-64.

[6] Lee JH, Khor TO, Shu L, Su ZY, Fuentes F, Kong AN. Dietary phytochemicals and cancer prevention: Nrf2 signaling, epigenetics, and cell death mechanisms in blocking cancer initiation and progression. *Pharmacol Ther* 2013; **137**(2): 153-171.

[7] Qu D, Shen L, Liu S, Li H, Ma YZ, Zhang RH, et al. Chronic inflammation confers to the metabolic reprogramming associated with tumorigenesis of colorectal cancer. *Cancer Biol* 2017; **18**(4): 237-244.

[8] Lin J, Feng J, Yang H, Yan Z, Li Q, Wei L, et al. Scutellaria barbata D. Don inhibits 5-fluorouracil resistance in colorectal cancer by regulating PI3K/AKT pathway. *Oncol Rep* 2017; **38**(4): 2293-2300.

[9] Sui H, Zhou LH, Yin PH, Wang Y, Fan ZZ, Li Q. JNK signal transduction pathway regulates MDR1/P-glycoprotein-mediated multidrug resistance in colon carcinoma cells. *World Chinese J Digestol* 2011; **19**: 892-898.

[10]Qin K, Chen K, Zhao W, Zhao X, Luo J, Wang Q, et al. Methotrexate combined with 4-Hydroperoxycyclophosphamide downregulates multidrug-resistance P-glycoprotein expression induced by methotrexate in rheumatoid arthritis fibroblast-like synoviocytes *via* the JAK2/STAT3 Pathway. *J Immunol Res* 2018; **2018**: 3619320.

[11]Akira S, Nishio Y, Inoue M, Wang XJ, Wei S, Matsusaka T, et al. Molecular cloning of APRF, a novel IFN-stimulated gene factor 3 p91-related transcription factor involved in the gp130-mediated signaling pathway. *Cell* 1994; **77**(1): 63-71.

[12]Yu H, Lee H, Herrmann A, Buettner R, Jove R. Revisiting STAT3 signalling in cancer: new and unexpected biological functions. *Nat Rev Cancer* 2014; **14**(11): 736-746.

[13]Wang Y, Shen Y, Wang S, Shen Q, Zhou X. The role of STAT3 in leading

the crosstalk between human cancers and the immune system. *Cancer Lett* 2018; **415**: 117-128.

[14]Spitzner M, Roesler B, Bielfeld C, Emons G, Gaedcke J, Wolff HA, et al. STAT3 inhibition sensitizes colorectal cancer to chemoradiotherapy *in vitro* and *in vivo*. *Int J Cancer* 2014; **134**(4): 997-1007.

[15]Jung SN, Shin DS, Kim HN, Jeon YJ, Yun J, Lee Yj, et al. Sugiol inhibits STAT3 activity *via* regulation of transketolase and ROS-mediated ERK activation in DU145 prostate carcinoma cells. *Biochem Pharmacol* 2015; **97**(1): 38-50.

[16]Yue P, Lopez-Tapia F, Paladino D, Li Y, Chen CH, Namanja AT, et al. Hydroxamic acid and benzoic acid-based STAT3 inhibitors suppress human glioma and breast cancer phenotypes *in vitro* and *in vivo*. *Cancer Res* 2016; **76**(3): 652-663.

[17]Wu S, Qiu Y, Shao Y, Yin S, Wang R, Pang X, et al. Lycorine displays potent antitumor efficacy in colon carcinoma by targeting STAT3. *Front Pharmacol* 2018; **9**: 881.

[18] Hou S, Yw YI, Kang HJ, Zhang L, Kim HJ, Kong Y, et al. Novel carbazole inhibits phospho-STAT3 through induction of protein-tyrosine phosphatase PTPN6. *J Med Chem* 2014; **57**(15): 6342-6353.

[19] Zhang W, Guo J, Li S, Ma T, Xu D, Han C, et al. Discovery of monocarbonyl curcumin-BTP hybrids as STAT3 inhibitors for drug-sensitive and drug-resistant breast cancer therapy. *Sci Rep* 2017; **7**: 46352.

[20]Liao YH, Lin CC, Lai HC, Chiang JH, Lin JG, Li TC. Adjunctive traditional Chinese medicine therapy improves survival of liver cancer patients. *Liver Int* 2016; **35**: 2595-2602.

[21]Liu, HZ, Liu H, Zhou ZY, Parise RA, Chu E, Schmitz JC. Herbal formula Huang Qin Ge Gen Tang enhances 5-fluorouracil antitumor activity through modulation of the E2F1/TS pathway. *Cell Commun Signal* 2018; **16**: 7.

[22]Chen MH, May BH, Zhou IW, Charlie CL, Zhang AL, Anthony L. FOLFOX 4 combined with herbal medicine for advanced colorectal cancer: a systematic review. *Phytother Res* 2014; **28**(7): 976-991.

[23]Zhang P, Lai ZL, Chen HF, Hang MZ, Wang A, Jia T, et al. Curcumin synergizes with 5-fluorouracil by impairing AMPK/ULK1-dependent autophagy, AKT activity and enhancing apoptosis in colon cancer cells with tumor growth inhibition in xenograft mice. *J Exp Clin Cancer Res* 2017; **36**(1): 190-201.

[24]Yao N, Ren K, Wang Y, Jin Q, Lu X, Lu Y, et al. Paris polyphylla suppresses proliferation and vasculogenic mimicry of human osteosarcoma cells and inhibits tumor growth *in vivo*. *Am J Chin Med* 2017; **45**: 575-598.

[25]Zhang JQ, Xia L, Fu NG, Liu MS, Tan YF. Systemic exposure of quercetin after administration of feng-liao-chang-wei-kang granules to rats. *J Ethnopharmacol* 2011; **133**(2): 911-913.

[26]Jia MD, Lu XF, Zhao LQ, Wang ZF, Zhang SS. Effects of Fengliao-Changweikang in diarrhea-predominant irritable bowel syndrome rats and its mechanism involving colonic motility. *J Neurogastroenterol Motil* 2018; **24**(3): 479-489.

[27]Amado NG, Predes D, Moreno MM, Carvalho IO, Mendes FA, Abreu JG. Flavonoids and Wnt/β-catenin signaling: potential role in colorectal cancer therapies. *Int J Mol Sci* 2014; **15**(7): 12094-12106.

[28]Theodoratou E, Kyle J, Cetnarskyj R, Farrington SM, Tenesa A, Barnetson R, et al. Dietary flavonoids and the risk of colorectal cancer. *Cancer Epidemiol Biomarkers Prev* 2007; **16**(4): 684-693.

[29]Cho YA, Lee J, Chang HJ, Sohn DK, Shin A, Kim J. Dietary Flavonoids, CYP1A1 Genetic Variants, and the risk of colorectal cancer in a Korean population. *Sci Rep* 2017; **7**(1): 128.

[30]Du WJ, Yang XL, Song ZJ, Wang JY, Zhang WJ, He X, et al. Antitumor activity of total flavonoids from daphne genkwa in colorectal cancer. *Phytother Res* 2016; **30**(2): 323-330.

[31]Yan Y, Wang L, He J, Liu P, Lv X, Zhang Y, et al. Synergy with interferon-lambda 3 and sorafenib suppresses hepatocellular carcinoma proliferation. *Biomed Pharmacother* 2017; **88**: 395-402.

[32]Wu YY, Zhang JH, Gao JH, Li YS. Aloe-emodin (AE) nanoparticles suppresses proliferation and induces apoptosis in human lung squamous carcinoma *via* ROS generation *in vitro* and *in vivo*. biochemical and communications. *Biochem Biophys Res Commun* 2017; **490**(3): 601-607.

[33]Saadatdoust Z, Pandurangan AK, Ananda Sadagopan SK, Mohd Esa N, Ismail A, Mustafa MR. Dietary cocoa inhibits colitis associated cancer: a crucial involvement of the IL-6/STAT3 pathway. *J Nutr Biochem* 2015; **26**(12): 1547-1558.

[34]Wang CZ, Zhang Z, Wan JY, Zhang CF, Anderson S, He X, et al. Protopanaxadiol, an active ginseng metabolite, significantly enhances the effects of fluorouracil on colon cancer. *Nutrients* 2015; **7**(2): 799-814.

[35]Yoshida M, Zhao L, Grigoryan G, Shim H, Gastrointestinal PH, Yun CC. Deletion of Na+/H+ exchanger regulatory factor 2 represses colon cancer progress by suppression of Stat3 and CD24. *Am J Physiol Gastrointest Liver Physiol* 2016; **310**(8): 586-598.

[36]Wei L, Zheng LP, Zhuang QC, Zhao JY, Cao ZY, Zeng JW, et al. Spica prunellae promotes cancer cell apoptosis, inhibits cell proliferation and tumor angiogenesis in a mouse model of colorectal cancer *via* suppression of stat3 pathway. *BMC Complement Altern Med* 2013; **13**: 144-153.

[37]Zhang WD, Guo JP, Li SS, Ma T, Xu DQ, Han C, et al. Discovery of monocarbonyl curcumin-BTP hybrids as STAT3 inhibitors for drug-sensitive and drug-resistant breast cancer therapy. *Sci Rep* 2017; **7**: 46352.

[38]Hengartner MO. The biochemistry of apoptosis. *Nature* 2000; **407**(6805): 770-776.

[39]Mariño G, Niso-Santano M, Baehrecke E, Kroemer G. Selfconsumption: the interplay of autophagy and apoptosis. *Nat Rev Mol Cell Biol* 2014; **15**(2): 81-94.

[40]Flusberg D, Sorger PP. Surviving apoptosis: life-death signaling in single cells. *Trends Cell Biol* 2015; **25**(8): 446-458.

[41]Wu S, Qiu Y, Shao Y, Yin S, Wang R, Pang X, et al. Lycorine displays potent antitumor efficacy in colon carcinoma by targeting STAT3. *Front Pharmacol* 2018; **9**: 881-891.

[42]Sharifi S, Barar J, Hejazi MS, Samadi N. Roles of the Bcl-2/Bax ratio, Caspase-8 and 9 in resistance of breast cancer cells to paclitaxel. *Asian Pac J Cancer Prev* 2014; **15**(20): 8617-8622.

[43]Wu B, Cui H, Peng X, Fang J, Zuo Z, Deng JJ, et al. Dietary nickel chloride induces oxidative stress, apoptosis and alters Bax/Bcl-2 and Caspase 3 mRNA expression in the cecal tonsil of broilers. *Food Chem Toxicol* 2014; **63**: 18-29.

[44]Li L, Wu WJ, Huang WJ, Hu G, Yuan WF, Li WF. NF-κB RNAi decreases the Bax/Bcl-2 ratio and inhibits TNF-α-induced apoptosis in human alveolar epithelial cells. *Inflamm Res* 2013; **62**(4): 387-397.

[45]Fernandes-Alnemri T, Takahashi A, Armstrong R, Krebs J, Fritz L, Tomaselli KJ, et al. Mch3, a novel human apoptotic cysteine protease highly related to CPP32. *Cancer Re* 1995; **55**(24): 6045-6052.